

# JOURNAL OF ADVANCED APPLIED SCIENCES

e-ISSN: 2979-9759



#### RESEARCH ARTICLE

# Structural and Electrical Properties of Al/ZnO<sub>NRs</sub>/ZnO/p-Si/Al Type MOS Diodes

Ahmet Tolga Taşçı<sup>1™</sup> 📵 • Merve Kızıldeniz<sup>2</sup> 📵 • Sedat Kurnaz<sup>3</sup> 📵 • Osman Çiçek<sup>1</sup> 📵

## ARTICLE INFO

### **Article History**

Received: 06.06.2023 Accepted: 22.06.2023 First Published: 30.06.2023

## Keywords

C-V  $G/\omega\text{-}V$  Hydrothermal method MOS diode SEM ZnO nanorod



#### ABSTRACT

In this study, Al/ZnO<sub>NRs</sub>/ZnO/p-Si/Al type MOS diodes with ZnO nanorods, synthesized by hydrothermal method, were fabricated. The fabricated devices were named as MD<sub>10-2</sub>, MD<sub>10-4</sub>, MD<sub>20-</sub> 2, MD<sub>20-3</sub> and MD<sub>20-4</sub> according to their molar concentration (mM) and the time they were kept in hydrothermal solution (hours). They were produced in different concentrations and times to optimize the electrical properties of the device. The basic electrical parameters of the fabricated structures were investigated by capacitance-voltage (C-V) and conductance-voltage (G/ω-V) measurements at a frequency of 10 kHz at room temperature. The C<sup>-2</sup> -V curves obtained from these measurements were used to calculate parameters such as the breakdown voltage (V<sub>o</sub>), zero-supply potential barrier height ( $\Phi_{Bo}$ ), depletion layer width ( $W_D$ ). Looking at the C-V curves for all structures, it was clearly seen that the aggregation, depletion and reversal regions were formed on the MOS-type diodes. In addition, the effect of interfacial states and series resistance (Rs) were analyzed from the curves. At the same time, the voltage dependent Rs values of MOS type diodes were calculated using the admittance method. According to the calculated data, it was observed that the lower series resistance value was found in MD<sub>10-2</sub> with low molar concentration and time. For this reason, it was said that the effect of interfacial states decreased in the MD<sub>10-2</sub> device compared to other structures. Finally, the diameter and arrangement of the nanorods were examined by scanning electron microscopy (SEM) of the MOS type diodes. SEM images showed the formation of well-aligned ZnO nanorods for all the fabricated structures.

## Please cite this paper as follows:

Taşçı, A. T., Kızıldeniz, M., Kurnaz, S., & Çiçek, O. (2023). Structural and electrical properties of Al/ZnO<sub>NRs</sub>/ZnO/p-Si/Al type MOS diodes. *Journal of Advanced Applied Sciences*, 2(1), 22-29. https://doi.org/10.29329/jaasci.2023.562.03

# 1. Introduction

The metal-oxide-semiconductor (MOS) structure was first proposed in 1959 by Moll, Pfann and Garrett as a voltage-controlled varistor (Sze et al., 2021). In 1960, Ligenza and Spitzer (1960) thermally grown silicon dioxide (SiO<sub>2</sub>) on Si semiconductor. This groundbreaking experimental success immediately led to the first report of the Metal-oxide-semiconductor field effect transistor (MOSFET) by Kahng and

Atalla (Sze et al., 2021). The MOS structure, which is used as an energy storage in electronic circuits due to the dielectric properties of the oxide layer in its structure, is the basic structure of modern semiconductor technology (Ohring, 1992; Saghrouni et al., 2015).

Zinc oxide (ZnO) is widely used for sensor and optoelectronic device applications due to its wide direct energy band gap (3.37 eV) and high exciton binding energy (60 MeV) at room temperature (30  $^{\circ}$ C) (Faraz et al., 2020; Demirezen et

E-mail address: atasci@kastamonu.edu.tr

<sup>&</sup>lt;sup>1</sup>Kastamonu University, Faculty of Engineering and Architecture, Department of Electrical and Electronics Engineering, Kastamonu/Türkiye

<sup>&</sup>lt;sup>2</sup>Eskişehir Technical University, Department of Aviation Electrical and Electronics, Eskişehir/Türkiye

<sup>&</sup>lt;sup>3</sup>Kastamonu University, Central Research Laboratory, Kastamonu/Türkiye

<sup>&</sup>lt;sup>™</sup> Corresponding author

al., 2021). Optoelectronic nanostructured materials have attracted attention due to their superior optical and electrical properties that enable their use in many technological applications (Faisal et al., 2020; Asvini et al., 2023). Recently, vertically oriented ZnO nanostructures in the form of nanorods have attracted increasing attention in applications such as solar cells, field effect transistors, etc. due to their many advantages such as the splitting direction of light absorption, large aspect ratios, low recombination rate (Shi et al., 2010; Yatskiv et al., 2014; Güler et al., 2023).

Yang et al. (2023) grew Co<sup>2+</sup> doped ZnO nanodispersed ZnO nanodispersions by hydrothermal method and obtained a structure with visible light photocatalysis and oil/water separation, providing a potential treatment strategy for industrial wastewater. Abutalib (2019) stated that the increase in dc and ac conductivities of nanocomposite samples obtained with ZnO nanorods of different diameters prepared by chemical vapor deposition (CVD) makes it a potential candidate for electrochemical device applications. Aspoukeh et al. (2022) discussed methods for the production of ZnO nanorods.

In this study, Al/ZnO<sub>NRs</sub> /ZnO/p-Si/Al type MOS diodes were fabricated by synthesizing ZnO nanorods on silicon semiconductor by hydrothermal method. In order to optimize the properties of the devices, different molar concentrations and times were used. The structural properties of ZnO NRs were investigated using scanning electron microscopy (SEM). Capacitance-voltage (C-V) and conductance-voltage (G/ $\omega$ -V) measurements of the fabricated MOS-type diodes were performed to obtain their electrical properties and the findings were discussed.

#### 2. Materials and Methods

To prepare Al/ZnO<sub>NRs</sub>/ZnO/p-Si/Al type MOS diodes, p-Si substrates with <100> surface orientation and 1-10  $\Omega$ .cm

resistivity were immersed in HF+ 20 H<sub>2</sub>O solution. They were then rinsed using deionized water with a resistivity of 18 M $\Omega$ . After cleaning, a 100 nm thick ZnO seed layer was deposited on the p-type Si substrate using RF sputtering technique under Ar:O<sub>2</sub> (80:20) gas pressure with 10 mTorr. The RF sputtering system was operated at 100 W and 50° C under a pressure of 1x10<sup>-6</sup> Torr. The substrates were then immediately annealed at 600° C for 30 minutes. A hydrothermal method was used to form ZnO nanorods on the seed layer. For this, two different solutions of 10 and 20 mM were prepared. They were immersed in 30 ml of growth solution consisting of deionized water containing zinc acetate dehydrate (Zn(CH<sub>3</sub>COO)<sub>2</sub>,2H<sub>2</sub>O) and hexamethylenetetetramine  $(C_6H_{12}N_4)$ equimolar concentrations (1:1). They were kept in an autoclave oven at 90° C for 2, 3 and 4 hours. The substrates were then dried in an oven at 90° C. SEM images of ZnO NR's, taken with 120000 magnification, with almost uniform size and 40-150 nm diameter are given in Figure 2. After ZnO nanorods were formed, high purity (99.999%) Al (100 nm thick) metal was coated on the backside of p-Si substrate using DC sputtering technique for ohmic contact. The ZnO<sub>NRs</sub>/ZnO/p-Si/Al devices were annealed at 450 ° C for 20 min to ensure low resistivity contact. Finally, 1 mm radius Al (100 nm) rectifier contacts were deposited onto the ZnO NR's using a DC sputtering system (Figure 1). The DC sputtering system is Ar gas with pressure 1x10<sup>-6</sup> Torr, partial pressure 40 mTorr, substrate rotation speed 10 rpm and DC power 135 W. The MOS diodes were classified as MD<sub>10-2</sub>, MD<sub>10-4</sub>, MD<sub>20-2</sub>, MD<sub>20-3</sub> and MD<sub>20-4</sub> according to molar concentration (mM) and time (h). Wayne Kerr 6500B instrument was used for capacitance-voltage and conductance-voltage measurements of the devices.

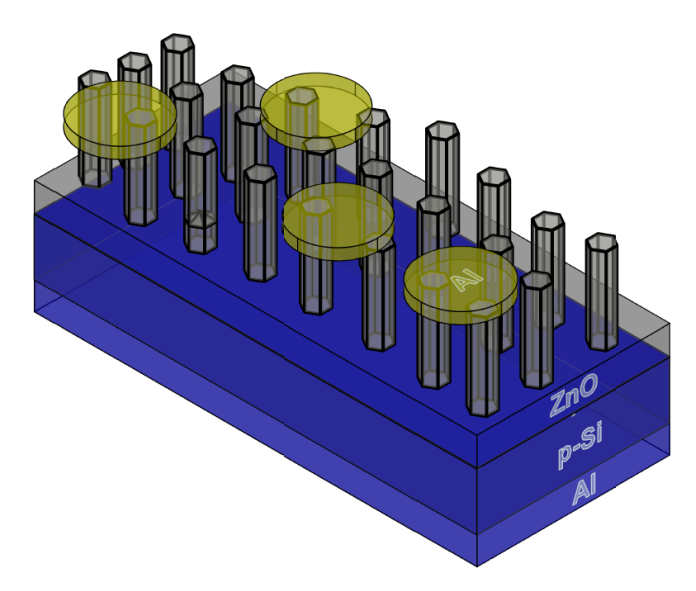


Figure 1. Al/ZnO<sub>NRs</sub> /ZnO/p-Si/Al MDs.



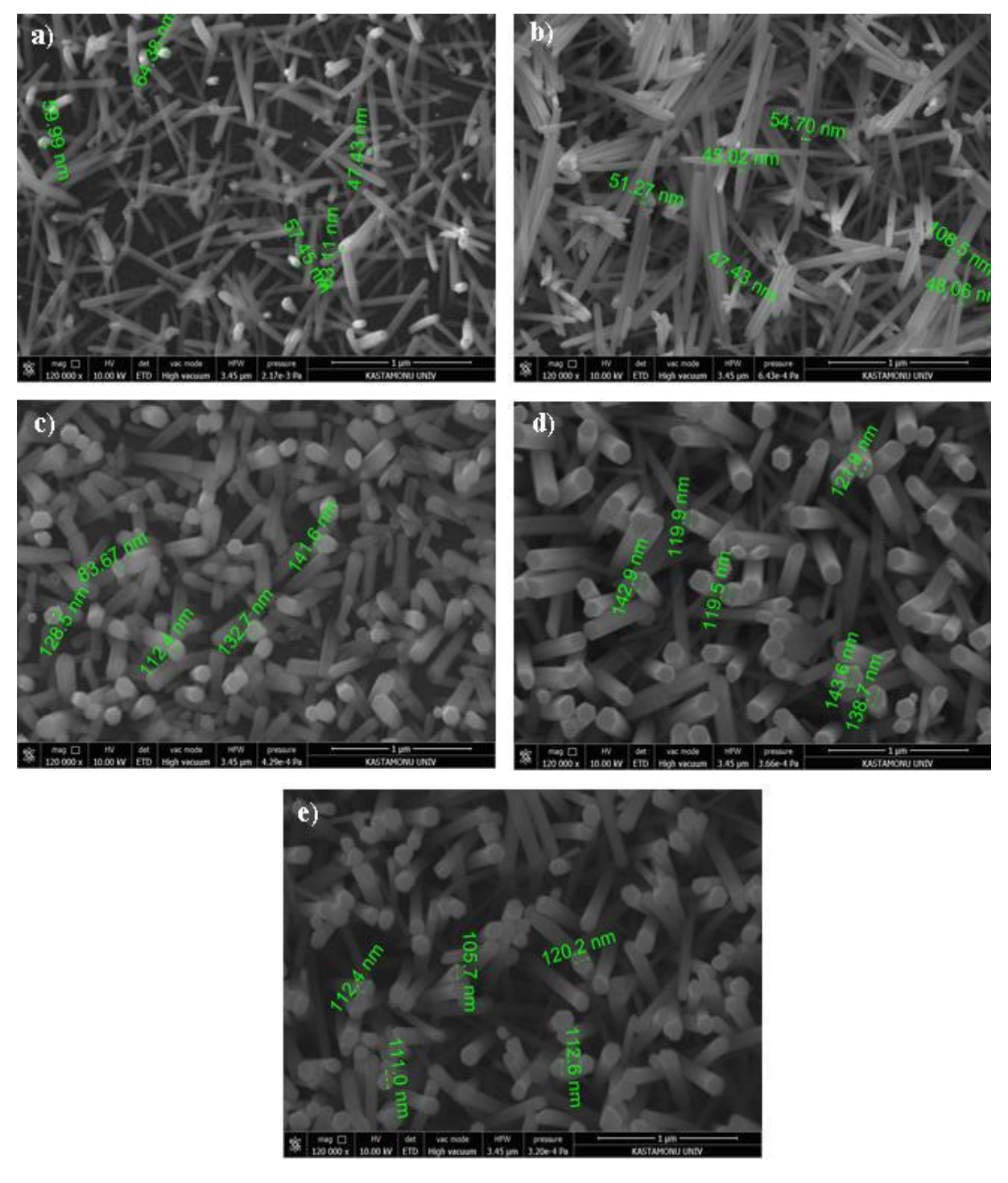


Figure 2. SEM images of ZnO nanorods a) MD10-2 b) MD10-4 c) MD20-2 d) MD20-3 e) MD20-4.

# 3. Results and Discussion

The capacitance-voltage (C-V) plots of  $Al/ZnO_{NRs}/ZnO/p-Si/Al$  type MOS diodes at a fixed frequency of 10 kHz at room temperature are given in Figure 3. C-V measurements are an important method to investigate the interfacial density of the MOS diode and its response to the applied frequency (Ashery et al., 2020). The C-V plots clearly show the regions of

accumulation, depletion and inversion of MOS structures (Grove & Grove, 1967). Although the behavior of the C-V curves is different for each sample, the accumulation regions are in the region of negative voltages and the reversal regions are in the region of positive voltages. The C-V curves show small and large peaks. These peaks indicate that the load flow in the device occurs in several stages (Al-Qrinawi et al., 2021).



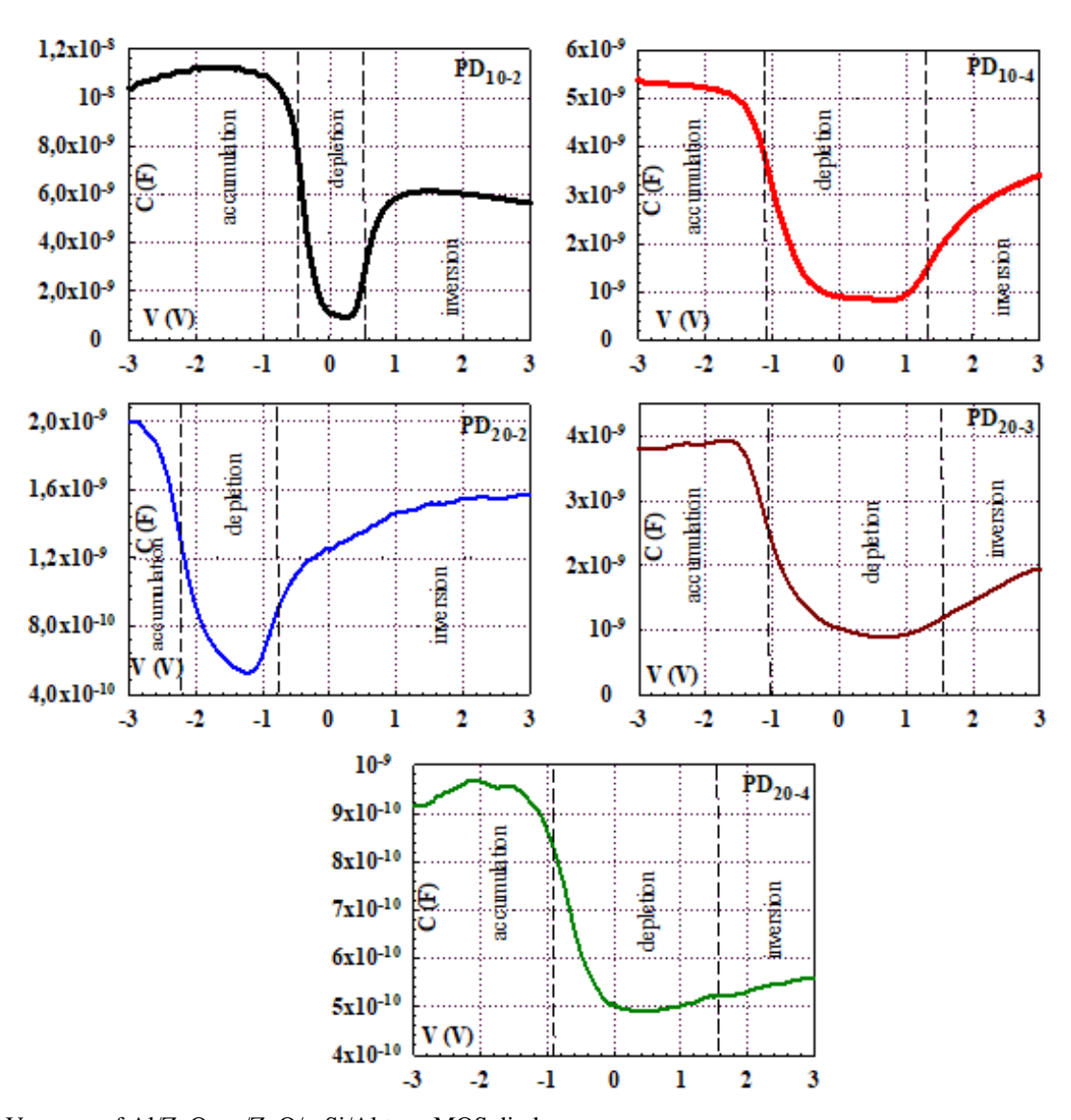


Figure 3. C-V curves of Al/ZnO<sub>NRs</sub> /ZnO/p-Si/Al type MOS diodes.

The change in the C values in the depletion region may be due to the reorganization of the interfacial states at the semiconductor-oxide interface, while the change in the C values in the inversion region may be caused by the effect of Rs. The effects of these factors should be minimized to improve the electrical properties of MOS diodes (Nicollian & Brews, 2002; Aldemir et al., 2020).

 $G/\omega\text{-V}$  curves of Al/ZnO<sub>NRs</sub>/ZnO/p-Si/Al type MOS diodes at a fixed frequency of 10 kHz at room temperature are given in Figure 4. It is seen from the graph that  $G/\omega\text{-V}$  curves depend on the applied voltage. The presence of peaks at the bias voltage of the C-V curves and  $G/\omega\text{-V}$  curves is generally attributed to the presence of the interfacial oxide layer in the structure, the ability of the interfacial states to follow the ac signal at low frequency and  $R_s$  (Demirezen et al., 2012).



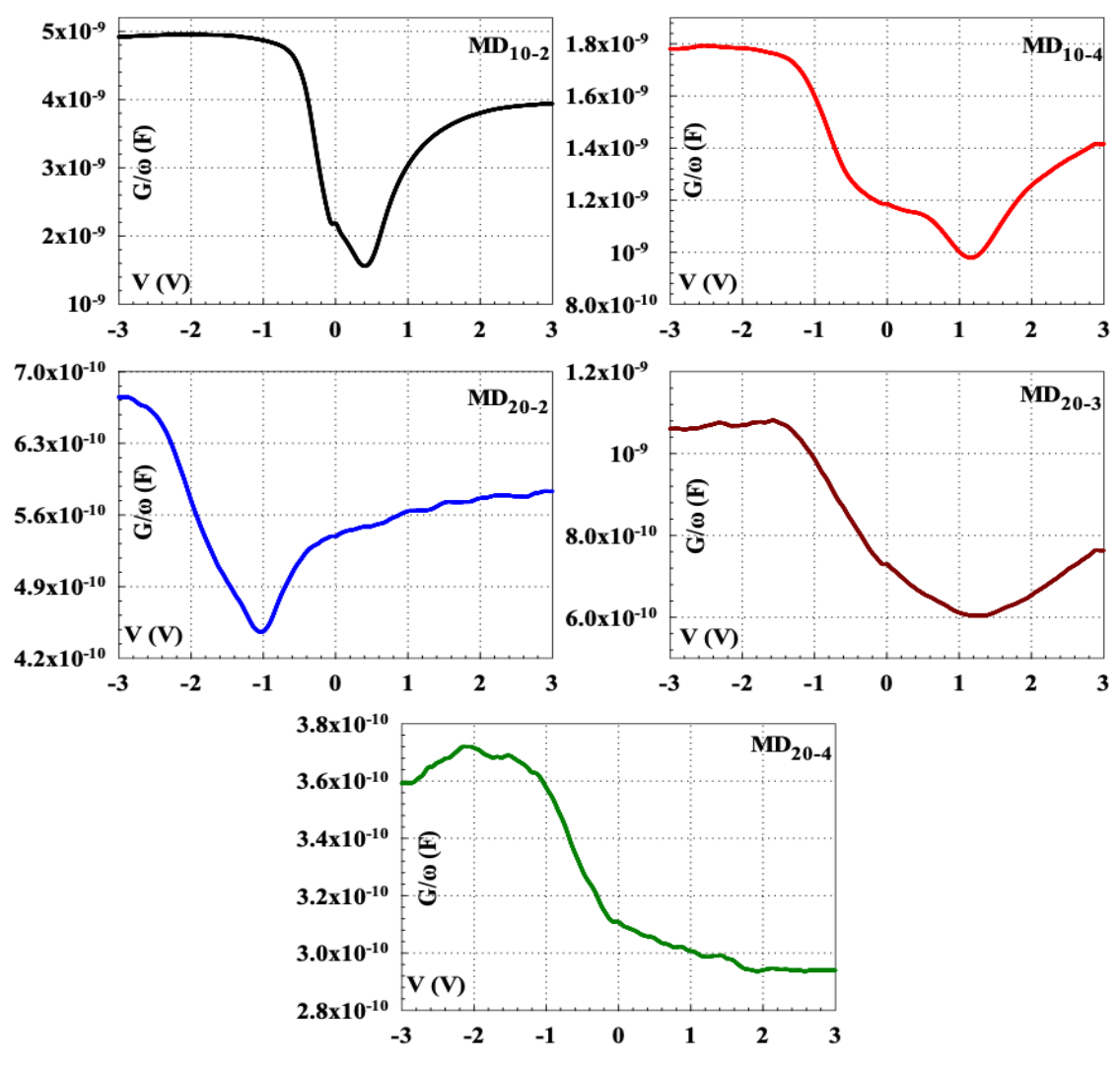
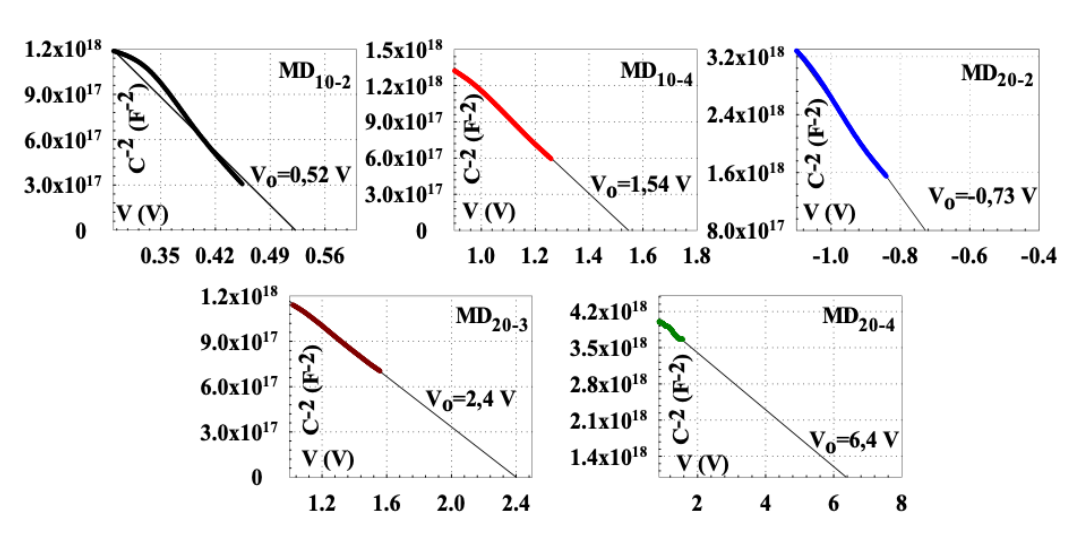


Figure 4.  $G/\omega$ -V curves of  $Al/ZnO_{NRs}$  /ZnO/p-Si/Al type MOS diodes.

C-V and  $G/\omega\text{-}V$  plots of MOS diodes show that they are highly voltage dependent. The voltage dependence is a function

of the Schottky barrier interface density of states and high series resistance (Parlaktürk et al., 2007).



**Figure 5.** C<sup>-2</sup> -V curves of Al/ZnO<sub>NRs</sub> /ZnO/p-Si/Al type MOS diodes.



 $C^{-2}$  -V plots of Al/ZnO<sub>NRs</sub> /ZnO/p-Si/Al type MOS diodes are given in Figure 5. The graphs show a good linear behavior for each structure. For a Schottky non-ideal diode, the inverse square of the reverse supply capacitance is a linear function of voltage (Sze et al., 2021).

$$C^{-2} = \frac{2(V_R + V_0)}{q\varepsilon_S\varepsilon_0 N_d A^2} \tag{1}$$

Here,  $V_R$  is the applied reverse bias voltage,  $V_o$  is the set-up voltage, q is the Boltmann constant,  $\varepsilon_s$  is the dielectric constant of p-Si semiconductor,  $\varepsilon_0$  is the dielectric constant of the cavity,  $N_D$  is the donor density, A is the area of the diode.

The zero feed potential barrier height  $\Phi_{\text{Bo}}$  is calculated from the following equation,

$$\Phi B(C-V) = V_0 + \frac{kT}{q} + E_F - \Delta_{\Phi B} = V_D + E_F - \Delta_{\Phi B}$$
 (2)

Here,  $V_D$  is the zero feed diffusion potential, kT/q is the thermal energy,  $\Delta_{\Phi B}$  is the image force barrier lowering and  $E_F$  is the Fermi energy level.

E<sub>F</sub> is obtained from the following equation,

$$E_F = \frac{kT}{q} \ln \left( \frac{N_C}{N_D} \right) \tag{3}$$

N<sub>C</sub> is the effective density of states in the conduction band of the semiconductor and is obtained from,

$$N_C = 4.82 \times 10^{15} T^{3/2} \left(\frac{m_e^*}{m_0}\right)^{3/2} \tag{4}$$

 $m_e^*$  is the effective electron mass,  $m_o$  is the free electron mass and  $m_e^*/m_o = 0.98$ .

 $\Delta_{\Phi B}$  is expressed by the following equation (Sze et al., 2021),

$$\Delta_{\Phi B} = \left[\frac{qE_m}{4\pi\varepsilon_{\varsigma}\varepsilon_{\rho}}\right]^{1/2} \tag{5}$$

E<sub>m</sub> maximum electric field is expressed by,

$$E_m = \left[\frac{2qN_D V_0}{\varepsilon_S \varepsilon_O}\right]^{1/2} \tag{6}$$

The electrical parameters obtained using the above equations for MOS diodes are given in Table 1. The increase in molar concentration also increased the barrier height. This is due to the increase in the density of interfacial states. It is clearly seen that  $MD_{20-2}$  exhibits a different behavior in terms of build-up voltage and barrier height. The shift of the set-up voltage to the negative region indicates that the oxide charges in the oxide layer are higher (Özben, 2007).

**Table 1.** Electrical parameters of Al/ZnO<sub>NRs</sub> /ZnO/p-Si/Al type MOS diodes obtained from C<sup>-2</sup> -V plot.

Sample	$N_D(cm^{-3})$	E <sub>F</sub> (eV)	$V_o(V)$	$\Phi_B(C-V)(eV)$	$\Delta_{\Phi B}(eV)$	$\mathbf{W}_{D}(\mathbf{cm})$	$E_{m}(V/cm) \\$
MD <sub>10-2</sub>	8,28x10 <sup>13</sup>	0,214	0,52	0,75	0,00615	3,02x10 <sup>-4</sup>	$3,45 \times 10^3$
$\mathrm{MD}_{10\text{-}4}$	$1,55 \times 10^{14}$	0,199	1,54	1,75	0,00944	3,79x10 <sup>-4</sup>	$8,11x10^3$
$MD_{20-2}$	$4,67x10^{13}$	0,228	-0,73	-0,48	0,00580	4,76x10 <sup>-4</sup>	$3,07x10^3$
MD <sub>20-3</sub>	$4,02x10^{14}$	0,175	2,40	2,58	0,01339	2,91x10 <sup>-4</sup>	$1,63 \times 10^4$
$MD_{20-4}$	$8,92x10^{14}$	0,155	6,4	6,56	0,02088	3,23x10 <sup>-4</sup>	$3,97x10^4$

There are many methods in the literature to calculate the series resistance values of MOS diodes. In this study, series resistance values are obtained by using the admittance method with the following equation (Norde, 1979; Özben, 2007; Al-Qrinawi et al., 2021).

$$R_S = \frac{G_m}{(G_m^2 + C_m^2 \omega^2)} \tag{7}$$

The capacitance and conductance values in the strong accumulation region are  $C_m$  and  $G_m$ , respectively. The  $R_s$ -V graph of  $Al/ZnO_{NRs}/ZnO/p$ -Si/Al type MOS diodes is given in Figure 6. In line with the data obtained, it is seen from the figure that the series resistance values of  $MD_{10-2}$  produced at low

molar concentration and time are lower compared to other structures. This indicates that the interfacial states for  $MD_{10-2}$  are reduced and the electrical properties of the device are improved. However, a thicker oxide layer can lead to a larger series resistance (Şenarslan et al., 2020).

It is seen that the voltage dependent  $R_s$  values give peaks in the  $\pm 1$  V range except  $MD_{20\text{-}2}$ . The peak values of  $MD_{20\text{-}2}$  are in the negative voltage region. This behavior of  $R_s$  is attributed to the restructuring and rearrangement of interfacial states localized between the semiconductor-oxide and in the forbidden energy range (Sze et al., 2021).



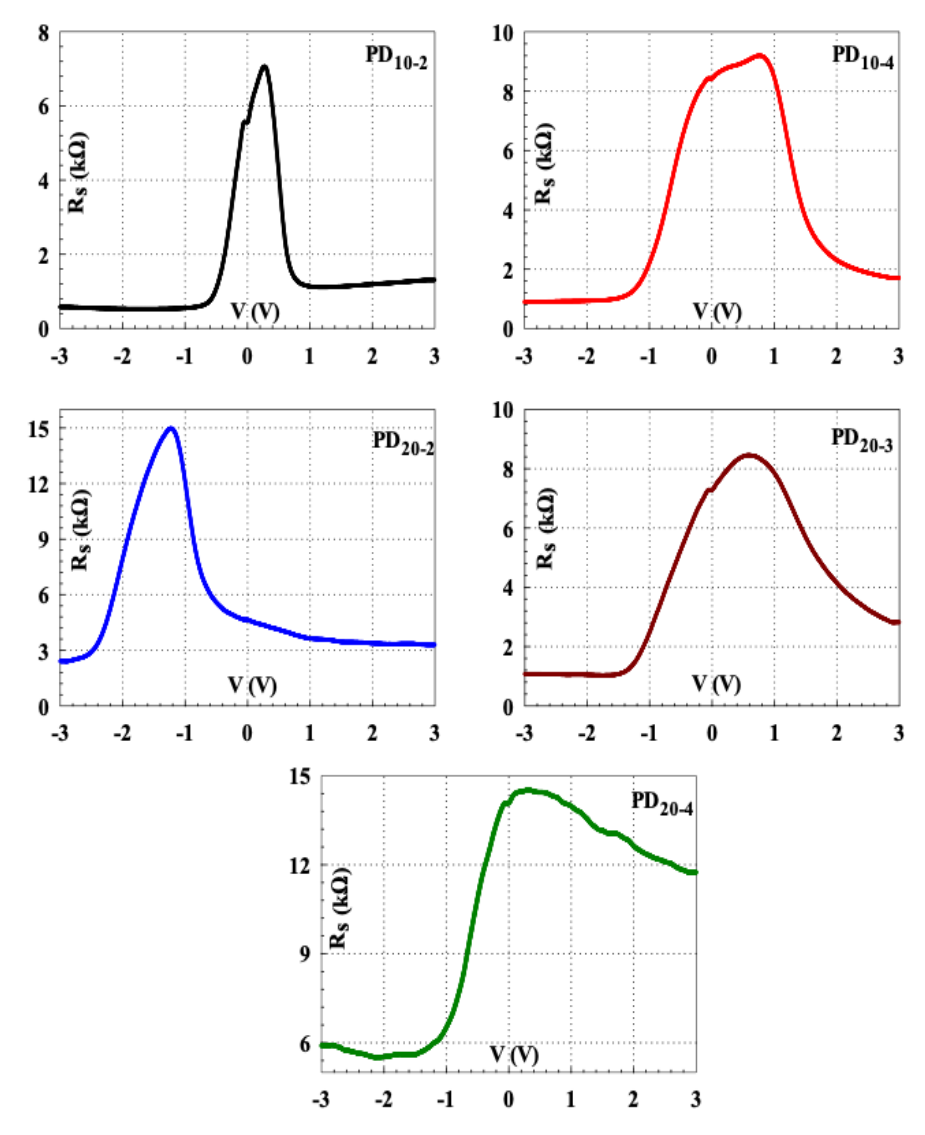


Figure 6. R<sub>s</sub> -V curves of Al/ZnO<sub>NRs</sub> /ZnO/p-Si/Al type MOS diodes.

## 4. Conclusion

capacitance and conductivity values Al/ZnO<sub>NRs</sub>/ZnO/p-Si/Al MOS type diodes consisting of hydrothermally grown ZnO nanorod arrays were measured at  $\pm 3$  V and 10 kHz frequency. C-V and G/ $\omega$ -V graphs were obtained from the measurement results. Some basic electrical parameters of MOS type diodes were calculated from C<sup>-2</sup> -V graphs. From the results, it was observed that the values of breakdown voltage V<sub>o</sub> and barrier height Φ<sub>B</sub> increased with increasing molar concentration. The MD<sub>20-2</sub> sample, on the other hand, exhibited a different behavior and the drying voltage shifted to the negative voltage region. This was attributed to the higher oxide charges in the oxide layer. The Rs-V characteristics of the MOS type diodes were also obtained using the admittance method. The results show that ZnO nanorods are significantly grown and well aligned by the hydrothermal method. It is also observed that the increase in molar concentrations for nanorod fabrication and the residence

time in the hydrothermal solution significantly affect the performance of MOS-type diodes.

# **Conflict of Interest**

The authors declare that they have no conflict of interest.

### References

Abutalib, M. M. (2019). Effect of zinc oxide nanorods on the structural, thermal, dielectric and electrical properties of polyvinyl alcohol/carboxymethyle cellulose composites. *Physica B: Condensed Matter*, 557, 108-116. https://doi.org/10.1016/j.physb.2019.01.018

Aldemir, D. A., Lapa, H. E., Özdemir, A. F., & Nazım, U. Ç. A. R. (2020). Doğal oksit arayüzey tabakalı Zr/p-Si schottky diyotlarının yüksek frekanslarda kapasitegerilim ve iletkenlik-gerilim karakteristiklerinin analizi. *Bitlis Eren Üniversitesi Fen Bilimleri Dergisi*, *9*(3), 1024-1030. https://doi.org/10.17798/bitlisfen.655179



- Al-Qrinawi, M. S., El-Agez, T. M., Abdel-Latif, M. S., & Taya, S. A. (2021). Capacitance-voltage measurements of hetero-layer OLEDs treated by an electric field and thermal annealing. *International Journal of Thin Film Science and Technology*, 10, 217-226. https://doi.org/10.18576/ijtfst/100311
- Ashery, A., Shaban, H., Gad, S. A., & Mansour, B. A. (2020). Investigation of electrical and capacitance-voltage characteristics of GO/TiO2/n-Si MOS device. *Materials Science in Semiconductor Processing*, 114, 105070. https://doi.org/10.1016/j.mssp.2020.105070
- Aspoukeh, P. K., Barzinjy, A. A., & Hamad, S. M. (2022). Synthesis, properties and uses of ZnO nanorods: a mini review. *International Nano Letters*, *12*(2), 153-168. https://doi.org/10.1007/s40089-021-00349-7
- Asvini, V., Saravanan, G., Kalaiezhily, R. K., & Ravichandran, K. (2023). Preparation and characterization of SbAs nanorods for opto-electronics applications. *Bulletin of Materials Science*, 46(1), 1-7. https://doi.org/10.1007/s12034-022-02849-4
- Demirezen, S., Sönmez, Z., Aydemir, U. M. U. T., & Altındal, Ş. (2012). Effect of series resistance and interface states on the I–V, C–V and G/ω–V characteristics in Au/Bidoped polyvinyl alcohol (PVA)/n-Si Schottky barrier diodes at room temperature. *Current Applied Physics*, *12*(1), 266-272. https://doi.org/10.1016/j.cap.2011.06.016
- Demirezen, S., Çetinkaya, H. G., Kara, M., Yakuphanoğlu, F., & Altındal, Ş. (2021). Synthesis, electrical and photosensing characteristics of the Al/(PCBM/NiO: ZnO)/pSi nanocomposite structures. *Sensors and Actuators A: Physical*, 317, 112449. https://doi.org/10.1016/j.sna.2020.112449
- Faisal, A. D., Ismail, R. A., Khalef, W. K., & Salim, E. T. (2020). Synthesis of ZnO nanorods on a silicon substrate via hydrothermal route for optoelectronic applications. *Optical and Quantum Electronics*, 52(4), 212. https://doi.org/10.1007/s11082-020-02329-1
- Faraz, S. M., Shah, W., Alvi, N. U. H., Nur, O., & Wahab, Q. U. (2020). Electrical characterization of Si/ZnO nanorod PN heterojunction diode. *Advances in Condensed Matter Physics*, 2020, 1-9. https://doi.org/10.1155/2020/6410573
- Grove, A. S., & Grove, A. S. (1967). *Physics and technology of semiconductor devices*. John Wiley & Sons Incorporated.
- Güler, A. C., Antoš, J., Masař, M., Urbánek, M., Machovský, M., & Kuřitka, I. (2023). Boosting the photoelectrochemical performance of Au/ZnO nanorods by co-occurring gradient doping and surface plasmon modification. *International Journal of Molecular Sciences*, 24(1), 443. https://doi.org/10.3390/ijms24010443
- Ligenza, J. R., & Spitzer, W. G. (1960). The mechanisms for

- silicon oxidation in steam and oxygen. *Journal of Physics and Chemistry of Solids*, *14*, 131-136. https://doi.org/10.1016/0022-3697(60)90219-5
- Nicollian, E. H., & Brews, J. R. (2002). MOS (metal oxide semiconductor) physics and technology. John Wiley & Sons.
- Norde, H. (1979). A modified forward I-V plot for Schottky diodes with high series resistance. *Journal of Applied Physics*, *50*(7), 5052-5053. https://doi.org/10.1063/1.325607
- Ohring, M. (1992). The materials science of thin films. Academic Press.
- Özben, E. (2007). The effects of prior nitridation process of silicon surface and different metal gates on the capacitance voltage characteristics of Metal-Ta2O5-Si mos capacitor (Master's thesis, Izmir Institute of Technology).
- Parlaktürk, F., Agasiev, A., Tataroğlu, A., & Altindal, Ş. (2007). Current-voltage (IV) and Capacitance-voltage (CV) characteristics of Au/Bi4Ti3O12/SnO2 structures. *Gazi University Journal of Science*, 20(4), 97-102.
- Saghrouni, H., Jomni, S., Belgacem, W., Elghoul, N., & Beji, L. (2015). Temperature dependent electrical and dielectric properties of a metal/Dy2O3/n-GaAs (MOS) structure. *Materials Science in Semiconductor Processing*, 29, 307-314. https://doi.org/10.1016/j.mssp.2014.05.039
- Şenarslan, E., Güzeldir, B., & Sağlam, M. (2020). Effects of surface passivation on capacitance-voltage and conductance-voltage characteristics of Al/p-type Si/Al and Al/V2O5/p-type Si/Al diodes. *Journal of Physics and Chemistry of Solids*, 146, 109564. https://doi.org/10.1016/j.jpcs.2020.109564
- Shi, Y., Yang, Z., Cao, H., & Liu, Z. (2010). Controlled coriented ZnO nanorod arrays and m-plane ZnO thin film growth on Si substrate by a hydrothermal method. *Journal of Crystal Growth*, *312*(4), 568-572. https://doi.org/10.1016/j.jcrysgro.2009.11.045
- Sze, S. M., Li, Y., & Ng, K. K. (2021). *Physics of semiconductor devices*. John Wiley & Sons.
- Yang, Z., Zhang, J., Zhang, W., Zhou, Q., Shen, J., & Huang, Y. (2023). Stearic acid modified Co2+-doped ZnO: The construction of micro-nano structure for its superhydrophobic performance and visible-light photocatalytic degradation of methylene blue. *Journal of Cleaner Production*, 382, 135391. https://doi.org/10.1016/j.jclepro.2022.135391
- Yatskiv, R., Brus, V. V., Verde, M., Grym, J., & Gladkov, P. (2014). Electrical and optical properties of graphite/ZnO nanorods heterojunctions. *Carbon*, 77, 1011-1019. https://doi.org/10.1016/j.carbon.2014.06.017

